Sensors and Actuators B 140 (2009) 273–277

Contents lists available at ScienceDirect

Sensors and Actuators B: Chemical

journal homepage: www.elsevier.com/locate/snb

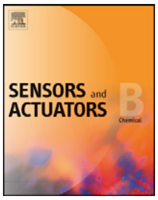

The study of the voltage drift in high-temperature proton conductor-based hydrogen sensors adopting the solid reference electrode

Young-Chang Yang*, Jinsu Park, Junwoong Kim, Angi Choi, C.O. Park

Department of Materials Science & Engineering, KAIST, Daejon 305-701, Republic of Korea

ARTICLE INFO

Article history:
Received 17 March 2009
Received in revised form 13 April 2009
Accepted 24 April 2009
Available online 7 May 2009

Keywords:
Hydrogen sensor
Titanium
n-type conductivity
Released protons

ABSTRACT

The long-term stability of the electrochemical hydrogen sensor comprised of the high-temperature proton conductor of $CaZr_{0.9}In_{0.1}O_{3-\delta}$ and the solid reference material of Ti/TiH_2/TiO mixture has been investigated. In the long-term stability test, the EMF drift of about 0.2–0.3 mV/h was observed. It may be caused by the extremely low oxygen partial pressure of 10^{-31} atm at 973 K evolved at the reference electrode due to the oxygen equilibrium reaction between TiO_2 and Ti_2O_3. It gives rise to n-type conduction at the reference electrode compartment, which then leads to a depletion of protons in the electrolyte as confirmed by the Raman spectra. The origin of the EMF drift is considered to result from the gradual increase in the hydrogen pressure at the reference compartment owing to the released protons from the electrolyte.

1. Introduction

Proton conductors with perovskite-type structure exhibit appreciable proton conduction under hydrogen-containing atmosphere at high temperatures [1–3]. Using these oxides as a solid electrolyte, various high-temperature hydrogen sensors had been constructed [4,5] for the measurement of dissolved hydrogen content in the Al melt. Among them, the sensors which replace the bulky gas reference compartment with a solid internal reference have been considered attractive.

In order to achieve a reliable performance of this type of sensor, many hydrogen sensors having an internal solid reference electrode have been studied so far. For example, Yajima et al. [6] have reported molecular sieve of $AlPO_4{\cdot}xH_2O$ and Zheng et al. [7–9] suggested metal/metal hydride mixture of Ca/CaH_2 for a reference material. Recently, Schwandt and co-workers [10,11] has extensively investigated other metal/metal hydride systems of titanium/titanium hydride, zirconium/zirconium hydride and neodymium/neodymium hydride. However these hydrogen sensors showed consistent results only for a short period of time but, in the long run, the cell voltage drifted markedly.

In this study, hydrogen sensor was made of titanium/titanium hydride mixture for an internal solid reference material and the high-temperature proton conductor of calcium zirconate doped with indium oxide, $CaZr_{1-x}In_xO_{3-\delta}$ for a solid electrolyte in an effort to investigate the origin of the lack of the long-term stability.

2. Experimental

The $CaZr_{1-x}In_xO_{3-\delta}$ solid electrolyte was prepared from 99.9% pure powders of $CaCO_3$(GCM-CF800, Korea), ZrO_2(Aldrich) and In_2O_3(Aldrich). The powders were weighted into appropriate ratios and mixed in a polypropylene jar with the aid of ethanol and zirconia balls for 12 h. It was dried and calcined at 1673 K in air for 10 h. The calcined powder was ball-milled in an ethanol solution for 24 h again and then identified the composition by X-ray diffraction. After drying and grinding, the powder was pressed into a grooved rectangular plate using a cold isostatic press of 250 MPa to fill the solid reference material. The pressed samples were then sintered at 1873 K for 10 h in air. The internal solid reference materials adopted in this experiment were the mixture of Ti and TiH_2 or Ti, TiH_2 and TiO. The internal reference material was encapsulated in a groove with the hermetic sealant, Dura Seal 1529 UHT (Cotronics Corp.) consisting of glass and ceramics. The sealant was heat-treated at 1173 K for 20 min. The schematic structure of the hydrogen sensor is illustrated in Fig. 1.

The EMF of the sensor was measured with a high impedance multimeter (>10G, Agilent 34970A) connected to a computer for the data collection. A mixture of hydrogen and nitrogen was used as a measuring gas and the total gas flow rate was fixed at 1000 cm^3/min. In order for the gas to be humidified, it was fed through water maintaining at a constant temperature of typically 23 °C, which corresponds to about 0.025 atm water partial pressure.

---

* Corresponding author. Tel.: +82 42 350 4258; fax: +82 42 350 3310.
E-mail addresses: yaruba22@kaist.ac.kr (Y.-C. Yang), eau4@kaist.ac.kr (J. Park), xentle1012@kaist.ac.kr (J. Kim), cergei@kaist.ac.kr (A. Choi), cops@kaist.ac.kr (C.O. Park).

0925-4005/$ – see front matter © 2009 Elsevier B.V. All rights reserved.
doi:10.1016/j.snb.2009.04.049

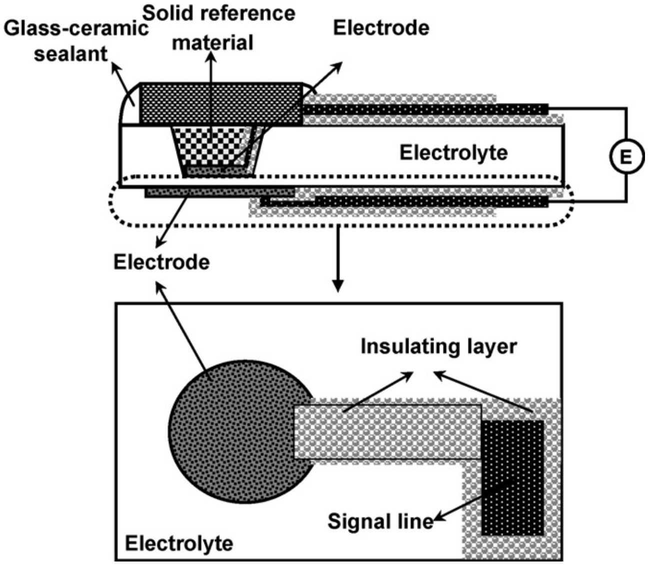

Fig. 1. Schematic view of the hydrogen sensor.

The partial electronic conductivity was measured by the Hebb–Wagner polarization method [12,16], where one electrode is nonreversible relative to the conducting ion of the electrolyte and another electrode is reversible as shown in Fig. 2. The structure of the Hebb–Wagner cell can be written as:

Glass–ceramic sealant | Porous Pt (ion-blocking electrode)

$$||\mathrm{CaZr}_{1-x}\mathrm{In}_x\mathrm{O}_{3-\delta}||\mathrm{PorousPt,\ hydrogengas(reversibleelectrode)} \qquad (1)$$

The polarization voltage applied to the Hebb–Wagner cell was in the range of 0.1–1.0 V supplied by a dc source (AUTOLAB/PGSTAT30) and the steady state currents were measured in dry 0.1 atm H_2 gas.

3. Results and discussion

EMF response of the sensor (2) was examined at temperatures ranging from 723 to 1173 K in a furnace where the hydrogen concentration was varied from 0.0005 to 0.1 atm as shown in Fig. 3.

$$\mathrm{Pt, H_2, Ti, TiH_2, TiO}|\mathrm{CaZr}_{1-x}\mathrm{In}_x\mathrm{O}_{3-\delta}|\mathrm{H_2, Pt} \qquad (2)$$

It is apparent from Fig. 3(a) that the 90% response time is less than 60 s and they give very stable behaviors for all temperatures tested. In addition, the dependence of the cell voltage on $\ln P_{H_2}[atm]$ was plotted in the range of 723–1173 K as shown in Fig. 3(b). It indicates that the sensor exhibits the Nernstian behavior of Eq. (3) with slopes larger than 95% of the theoretical value:

$$E = E_0 - \frac{RT}{2F} \ln\ P_{H_2}^{\mathrm{mea.}} \qquad (3)$$

where E_0, R, T and F are, $\Delta G^{\circ}_{TiH_2}/2F$, the universal gas constant, the absolute temperature, and the Faraday constant, respectively.

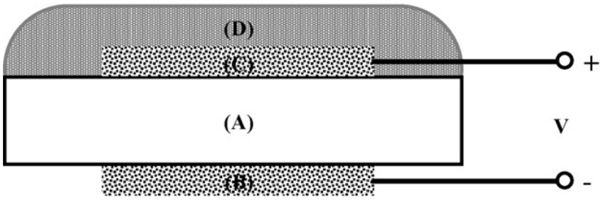

Fig. 2. Schematic view of the Hebb–Wagner polarization cell; (A) $CaZr_{1-x}In_xO_{3-\delta}$; (B) and (C) porous Pt; (D) glass–ceramic sealant.

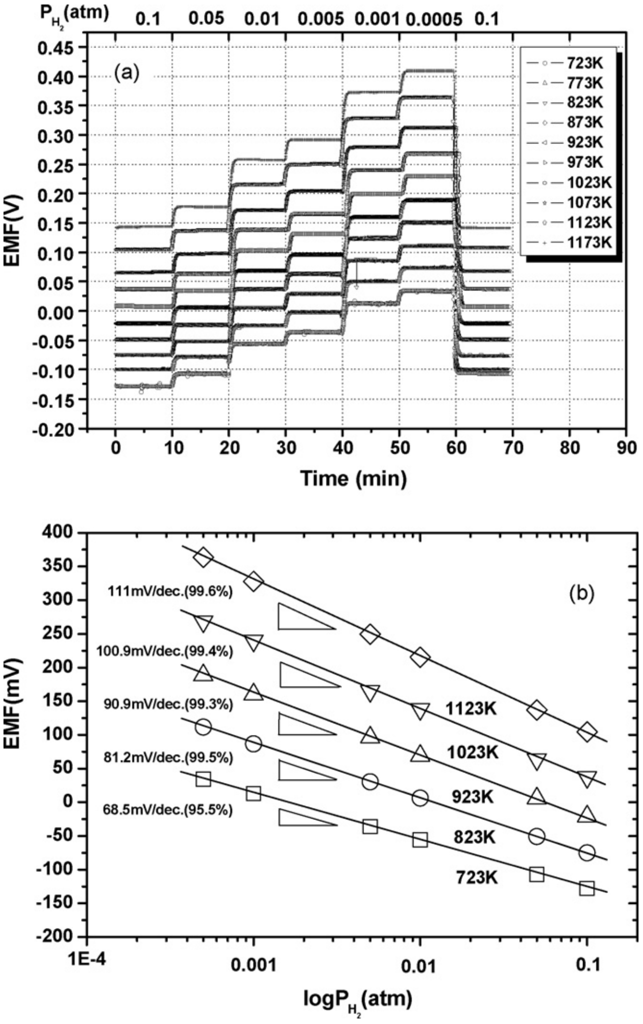

Fig. 3. EMF response of the hydrogen sensor at various temperatures: (a) transient behavior as a function of time for different H_2 pressures and (b) sensitivities.

However, it was found that the EMF started to increase with time after 6 h in operation with a rate of 0.25 mV/h as shown in Fig. 4(a). Interestingly, the old sensor exhibits the same slope with the new one in the cell voltage vs. $\ln P_{H_2}$ diagram even though E_0 increases with usage as shown in Fig. 4(b).

The oxygen activities at the reference electrode are compared for the Ti/TiH_2 and the $Ti/TiH_2/TiO$ reference mixtures which are hermetically encapsulated as shown in Fig. 2. Here, the hydrogen pressure expects to be fixed to 0.267 atm at 973 K by the chemical reaction (4):

$$\mathrm{Ti + H_2(g) = TiH_2} \qquad (4)$$

In principle, the oxygen pressure is thought to be floating for Ti/TiH_2 reference mixture. It may be affected by the oxygen trapped during the fabrication of the reference chamber. On the other hand, in the case of $Ti/TiH_2/TiO$ reference mixture, TiO is expected to play a role of fixing oxygen pressure by the chemical reaction (5):

$$\mathrm{Ti} + \tfrac{1}{2}\mathrm{O_2(g) = TiO} \qquad (5)$$

In order to predict the oxygen pressure-determining equilibrium in the reference compartment, the compositions of the reference mixtures for the old sensors are examined by the XRD analysis as shown in Fig. 5. It is noted that Ti, TiH_2, TiO_2, TiO and Ti_2O phases are found from the Ti/TiH_2 mixture while additional Ti_2O_3 peak appeared for the $Ti/TiH_2/TiO$ mixture when they are taken after